Applied Water Science (2021) 11:105
https://doi.org/10.1007/s13201-021-01442-0

ORIGINAL ARTICLE

Preparation of ZnO/Nylon 6/6 nanocomposites, their characterization and application in dye decolorization

Khalid Saeed[1,2] · Idrees Khan[2] · Madiha Ahad[1] · Tariq Shah[1] · Muhammad Sadiq[1] · Amir Zada[3] · Noor Zada[1]

Received: 14 March 2021 / Accepted: 27 May 2021 / Published online: 4 June 2021

Abstract

Nylon 6/6 and ZnO/nylon 6/6 nanocomposite films were prepared by solvent casting method. Morphological study displayed that ZnO NPs are better dispersed in nylon 6/6. However, some agglomerations were found by the incorporation of high quantities of fillers. The thermal stabilities of neat nylon 6/6 films decreased by addition of nanoparticles (NPs). DSC study shows that the NPs slow down the crystallization rate of neat polymer matrix. POM of Nylon 6/6 upon crystallization showed distinct sized spherulites, which decreased by the incorporation of NPs because of nucleation effect of NPs. The mechanical properties of neat polymer are decreased by addition of ZnO NPs, which might be due to agglomeration of fillers. The neat nylon 6/6 and ZnO/nylon 6/6 nanocomposite were used for the photodegradation of alizarin red (AR) dye, which shows that pure nylon 6/6 degraded about 28% dye while 30% ZnO/Nylon 6/6 degraded about 58.3% dye within 5 h irradiation.

Keywords Nanocomposite · Photodegradation · Nylon 6/6 · Nanoparticles · Alizarin red

Introduction

Nanocomposites are a class of new materials of multiple phases with a dispersed phase (fillers) having at least one dimensions in the nanometer scale (Murugesan and Scheibel 2020; Dunlop and Bissessur 2020). Polymer-based nanoparticle composite materials have received much attention due to their synergistic and hybrid properties. These polymer-based nanocomposite materials have exhibiting superior mechanical, thermal, electrical, optical and processing properties (Schmidt and Malwitz 2003; Garces et al. 2000). The reinforcement of NPs to polymers not just modifies its physical characteristics but also implement novel characteristics in the polymer (Hanemann and Szabo2010). Incorporating NPs also improve stiffness and the toughness of the polymers, which enhance their barrier properties and resistance to fire or ignition (Alexandre and Dubois 2000). These nanocomposites have wide range of applications in various fields such as military equipments, protective garments, safety, aerospace, automotive, electronics and optical devices (Jeon and Baek 2010). The enhancement of properties by NPs incorporation is due to either the ability of a group of NPs to act as charge carriers, electrooptically active centers, or as optical micro-cavities (Carter et al. 1997). Various fillers materials were used for polymer nanocomposite preparation such as CNTs (Saeed and Khan 2014; Irzhak et al. 2019), clay (Meneghetti and Qutubuddin 2006; Rezazadeh et al. 2020), silica (Khdary and Abdelsalam 2020; Ibrahim and Sultan2020), graphene (Li et al. 2016; Iniestra-Galindo et al. 2019; Ovcharenko et al. 2020) and metals NPs (Iwamoto et al. 2003; Jadhav et al. 2020; Ali et al. 2014, 2020).

Currently, the NPs have received huge attention due to their unique size-dependent properties (Kumar et al. 2013) and potential applications in various fields (Sinha et al. 2014). The NPs have size in the range between 1 and 100 nm. The unique and improved properties of NPs are due to their specific characteristics like size, distribution and morphology (Selvam and Sivakumar 2015). NPs usually present novel magnetic, electronic, optical, and chemical properties because of their very minute sizes

✉ Khalid Saeed
khalidkhalil2002@yahoo.com

✉ Idrees Khan
idreeschem_uom@yahoo.com

[1] Department of Chemistry, University of Malakand, Chakdara, Lower Dir, KP, Pakistan

[2] Department of Chemistry, Bach Khan University, Charsadda, KP, Pakistan

[3] Department of Chemistry, Abdul Wali Khan University, Mardan, KP, Pakistan

and huge surface areas. The metals oxides NPs have wide potential applications in the field of catalysis (Gopiraman et al. 2020), superconductors (Jasim et al. 2016), pigments (Magdassi et al. 2003), sensors (Hjiri 2020; Sovizi, Mirzakhanib 2020), adsorbents (Chatterjee et al. 2020), and magnetic resonance imaging (Mauri et al 2020; Wu et al. 2020). Currently transition metals NPs are employed as photocatalysts for the photodegradation of various organic pollutants. However, these photocatalysts are present in suspended forms and several difficulties have been observed such as its aggregation in bulk solution, their separation from solution after reaction and high recombination rate of the photogenerated electron–hole pairs (Soltani and Haghighat 2016).

In the present study, zinc oxide nanoparticles (ZnO NPs) were synthesized via chemical reduction technique and employed as fillers in Nylon 6/6 in order to avoid the above mentioned disadvantages. Nylon 6/6 has high hydrophilicity and thermal stability and great tensile strength (Halim et al. 2019). Nylon 6/6 is applied as a potential material in different fields for different purposes such as in cement for properties enhancement (Tri et al. 2020), lithium-ion batteries (Yanilmaz et al. 2017), antibacterial agents (Xu et al. 2015), adsorbents (Parlayici et al. 2019), etc. ZnO NPs not only affected the various properties of the Nylon 6/6 but too employed as photocatalyst for the photodegradation of Alizarin red dye. ZnO NPs have received great attention because of their unique catalytic, optical, electrical and electronic properties and as well as their low cost and possible applications in diverse areas (Ansari and Mohammad 2016). ZnO semiconductors have similar bandgap as TiO_2 (Wang et al. 2007). ZnO materials are reported for the photodegradation of dyes (Długosz and Banach 2021), pesticides (Russo et al. 2021), antibiotics (He et al. 2019), volatile organic compounds (Nagaraju et al. 2020), surfactants (Huszla et al. 2021), etc. Various polymer-metal nanocomposite are reported in literature as a catalyst/photocatalyst such as Ag/Pd Nanoparticle-Loaded Poly(ethylene imine) Composite (Feng et al. 2020), cobalt–manganese oxides/nylon 6,6 nanocomposites(Saeed et al. 2018), ZnO/PMMA nanocomposites(Mauro et al. 2017), Polypropylene/ZnO Nanocomposites(Prasert et al. 2020), FeNiSe-Chitosan microspheres(Yang et al. 2021), ternary ferrites-chitosan nanocomposite (Nawaz et al. 2020), etc. In our study, ZnO/nylon 6/6 is reported for the first time as a photocatalyst for the photodegradation of alizarin red dye. Alizarin red is reported to be carcinogenic and mutagenic probably because it could induce oxidative damages in organisms (Hu et al. 2019). Its acute toxicity leads to irritation to eyes, skin, lungs, mucous membranes and gastrointestinal tract while in chronic conditions it leads to dermatitis (Rehman and Mahmud 2013).

Experimental work

Materials

Nylon 6/6 was obtained from Aldrich. The formic acid was obtained from Sigma Aldrich, while Alizarin red dye was received from Scharlau (S L Spain). Sodium hydroxide and Zinc chloride were supplied by Scharlau Chemicals.

Preparation of ZnO particles

0.1 M $ZnCl_2$ (100 mL) solution was taken in a flask, and sodium hydroxide (0.2 M) solution was added slowly into the solution under constant stirring until pH become basified (pH 9). The reaction mixture was heated for 2 h at 60 °C in oil bath with constant stirring. After heating, the solution was cooled to room temperature and filtered. The obtained precipitates were washed several times with distilled water in order to neutralize it and remove any attached impurities and then oven dried at 120 °C for overnight.

Preparation of nanocomposite films

First of all, nylon 6/6 was dissolved in formic acid through stirring and then known quantity of ZnO was incorporated to the Nylon 6/6 solution. The obtained mixture was sonicated (full volume at room temperature) through sonicator for 30 min for the complete dispersion of ZnO NPs in polymer solution. The nanocomposite sheets (ZnO(2wt%)/nylon 6/6, ZnO(10wt%)/nylon 6/6, ZnO(20wt%)/nylon 6/6 and ZnO(30wt%)/nylon 6/6) were prepared through solution casting method. The prepared nanocomposite films were placed in distilled water in order to eliminate any attached chemicals. The ZnO/nylon 6/6 nanocomposites were dried in an oven at 60 °C and then stored. The same method is followed for the preparation of pure nylon 6/6 without adding ZnO NPs.

Photodegradation study

In dye degradation reaction, 0.01 g of nylon 6/6 or nanocomposites (small pieces) was added to 10 mL (1 g/L) alizarin red (200 ppm) in a beaker and then irradiated under UV light (254 nm, 15 w) for different irradiation time (1, 3 and 5 h). After particular irradiation time, the nylon 6/6 nanocomposites films were separated from the dye. The nanocomposites preparation and photodegradation study are represented in Fig. 1.The dye degradation studies were carried out using UV/Vis spectrometer (Model = Shimadzu 1800, Japan). The

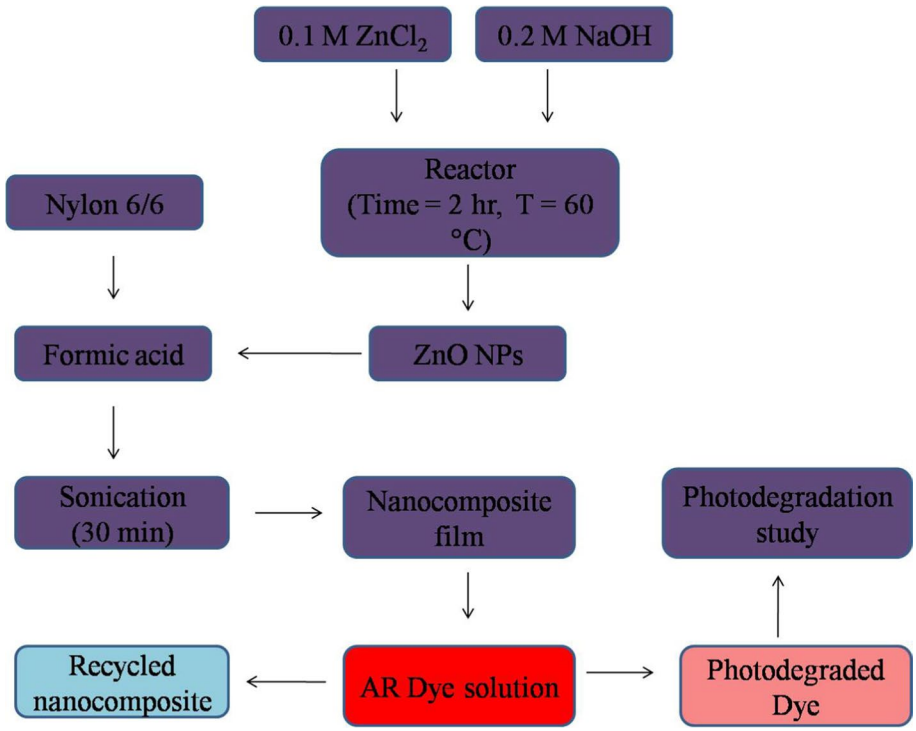

Fig. 1 Schematic diagram of nanocomposite preparation and AR dye degradation study

%degradation of dye was calculated using the following equations (Saeed et al. 2015).

$$\text{Degradation rate } (\%) = \left(\frac{C_0 - C}{C_0}\right) \times 100 \quad (1)$$

$$\text{Degradation rate } (\%) = \left(\frac{A_0 - A}{A_0}\right) \times 100 \quad (2)$$

where C_0 is the initial dye concentration, C is the dye concentration after UV irradiation, A_0 shows initial absorbance, and A shows the dye absorbance after UV irradiation.

Instrumentation

The prepared neat nylon 6/6 and ZnO/nylon 6/6 nanocomposite were characterized through scanning electron microscopy (JEOL, JSM-5910, Japan). The TG/DTA thermograms of neat nylon 6/6 and ZnO/nylon 6,6 nanocomposite were obtained in a nitrogen atmosphere at a heating rate of 20 °C/min from room temperature to 700 °C using a TGA (Perkin Elmer). The mechanical properties of neat nylon 6/6 and ZnO/nylon 6,6 nanocomposite were investigated by UTM (Model 100-500 KN, Iestomeric Inc. UK). The POM study was performed using polarized optical microscope (Optika B-600). In POM analysis, sample was melted in a heater and squeezed between two glass slides for 10 min. The photodegradation study of alizarin red was monitored using UV-visible spectrophotometer (UV-1800, Shimadzu, Japan).

Results and discussion

SEM study

SEM images of cross section of the neat nylon 6/6 and ZnO/nylon 6/6 are shown in Fig. 2. Figure 2a represented that neat nylon 6/6 has porous structure. Figure 2b and c represents the SEM images of 10 wt% ZnO/nylon 6,6 and 30 wt% ZnO/nylon 6,6, respectively. The SEM images of nanocomposites represented that the ZnO NPs (below 500 nm) were embedded well within the nylon 6/6. The NPs are found both in agglomerated and dispersed form inside the matrix. The aggregation of nanoparticles in the polymer generally takes place by addition of its high amount of inside the matrix.

Thermal properties

The TG thermograms of nylon 6/6 and nanocomposites are shown in Fig. 3. The thermogram of neat polymer remains unchanged up to 360 °C and then dropped quickly. The neat nylon6/6 completely degrades at 658 °C. The thermograms of nanocomposite illustrated that their thermal stability declined regularly as increased the quantity of ZnO NPs, which might be due to ZnO NPs, which work as catalyst during the decomposition of Nylon 6/6. Similarly, Xu et al. (Xu et al. 2006) also reported the lower degradation temperature in the case of SWCNTs/poly(vinylidene fluoride).

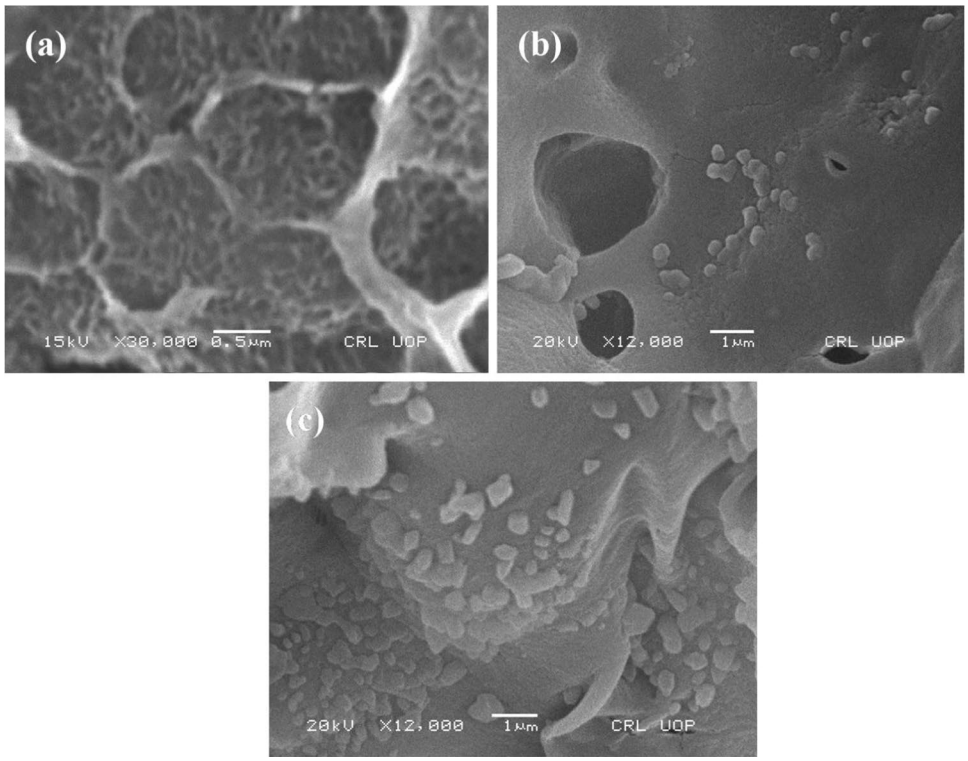

Fig. 2 SEM images of **a** neat nylon 6/6 **b** 10 wt% ZnO/nylon 6/6 and **c** 30 wt% ZnO/nylon 6/6

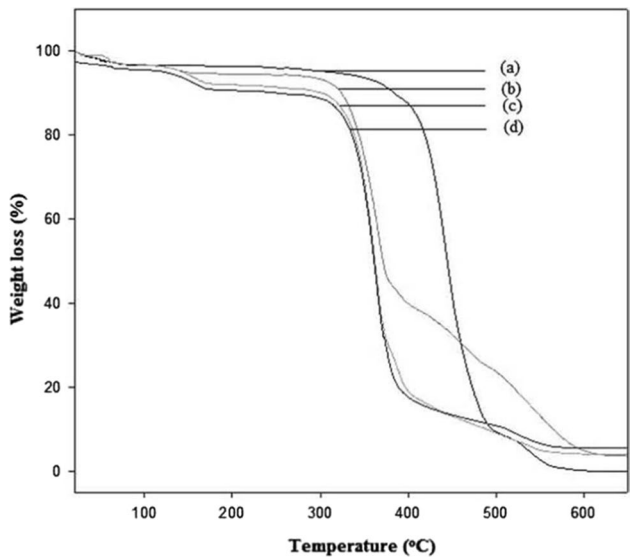

Fig. 3 TG thermograms of **a** nylon 6/6, **b** 10 wt% ZnO/nylon 6/6, **c** 20 wt% ZnO/nylon 6/6 and **d** 30 wt% ZnO/nylon 6/6

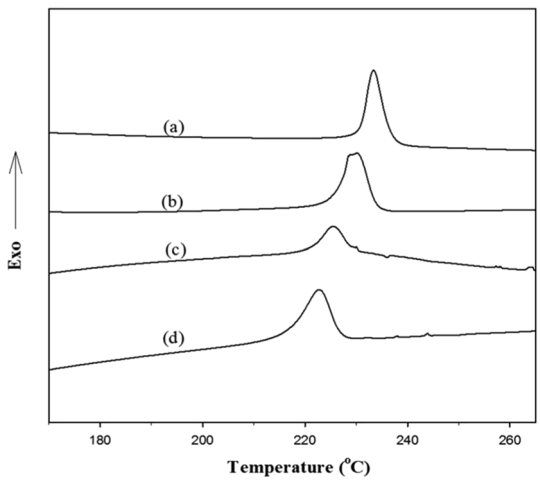

Fig. 4 DSC Tc of **a** nylon 6/6, **b** 10 wt% ZnO/nylon 6/6, **c** 20 wt% ZnO/nylon 6/6 and **d** 30 wt% ZnO/nylon 6/6

DSC study

The DSC crystallization temperature (Tc) of pure nylon 6/6 and its nanocomposites are presented in Fig. 4. The Tc of nylon 6/6 polymer was 233 °C, while the Tc of ZnO/nylon 6/6 was reduced slowly as the quantity of ZnO increased into the Nylon matrix (Fig. 4b–d). It indicates that ZnO slows down the crystallization rate of polymer. The Rajakumar and Nanthini also reported the decrease of Tc in case of montmorillonite/polycarbonate/PBT. They recommended that the low Tc means the slow rate of crystallization, which present that the montmorillonite act as the compatibilizers. The stronger interactions between the clay and polymer blend matrix limited the movements of chain and thus the rate of crystallization is slow down (Rajakumar and Nanthini 2013).

The DSC curves of second heating melting temperature (T_m) of nylon 6/6 and the nanocomposites are shown in Fig. 5. The both types of samples presented double melting temperature "peaks (Tm_1 and Tm_2). The T_{m1} and T_{m2} of nylon 6/6 were about 249 and 259 °C, respectively." The T_m peaks of nylon 6/6 were reduced as increased the ZnO NPs (Fig. 5b–d). The decrease in melting temperature in clay/PET nanocomposites was also reported by Bizarria et al. (Bizarria et al. 2007). They recommended that the nanoscale interactions between the matrix and clay surface results the creation of smaller amount stable crystals through the crystallization from the melting.

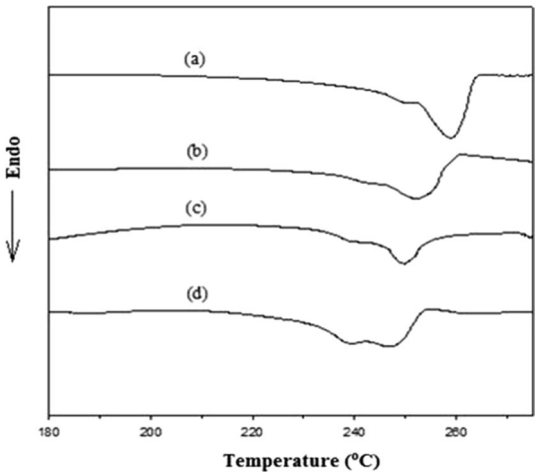

Fig. 5 DSC Tc of **a** nylon 6/6 **b** 10 wt% ZnO/nylon 6/6 **c** 20 wt% ZnO/nylon 6/6 and **d** 30 wt% ZnO/nylon 6/6

POM study

The POM images of nylon 6/6 and its nanocomposite are shown in Fig. 6. POM image of neat polymer showed distinct size crystalline spherulites (Maltese cross type). The size of spherulites of nylon 6/6 is within the range of 20–50 µm. Figure 6b–d presents the POM images of nanocomposites, which illustrated that the spherulites size of nanocomposites was reduced regularly as ZnO NPs are incorporated to nylon 6/6. The size reduction of spherulites was due to intermolecular interaction on crystallization behavior of polymer and NPs. The POM images also presented that the spherulites size of ZnO/nylon 6/6 is reduced at regular pattern as increased the amount of ZnO NPs. This decrease in spherulites sizes might be due to nucleation role of ZnO on nylon 6/6. Because of the colliding effect of the ZnO NPs, the growth of the nylon 6/6 spherulites is limited. On the other hand, the nucleation of ZnO NPs causes a large numbers of nucleuses, which results a huge number of spherulites in the limited space. Therefore, the perfect spherulites cannot form by the incorporation of high quantity of ZnO NPs.

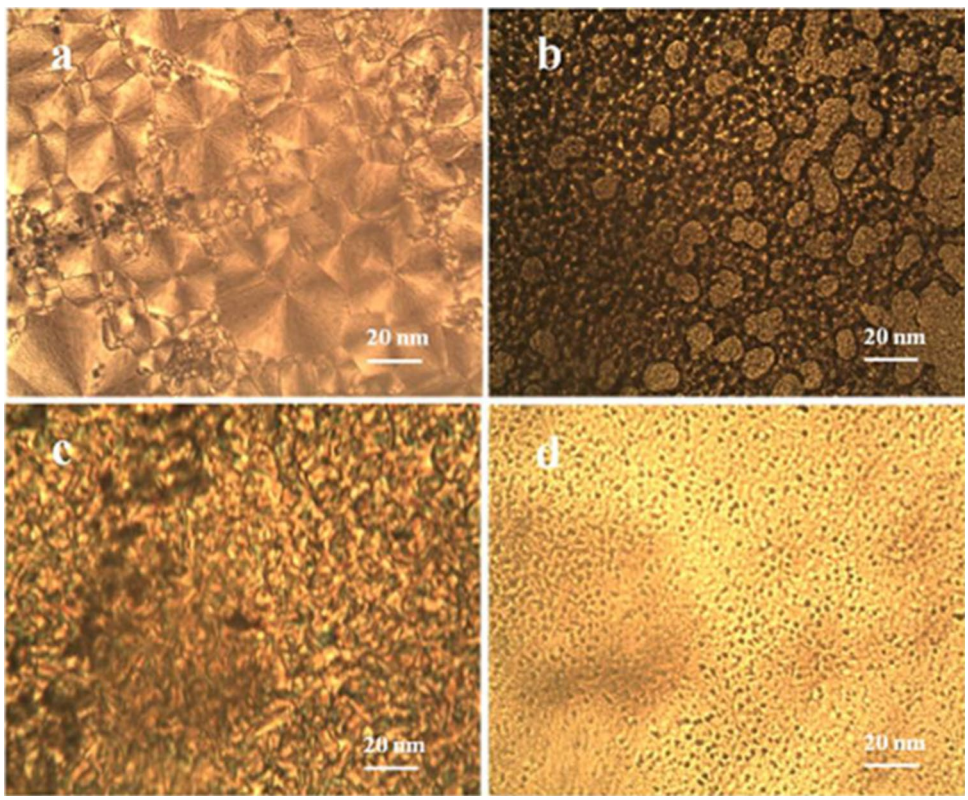

Fig. 6 POM micrographs of **a** nylon 6/6, **b** 10 wt% ZnO/nylon 6/6, **c** 20 wt% ZnO/nylon 6/6 and **d** 30 wt% ZnO/nylon 6/6

Table 1 Mechanical properties of neat polymer and ZnO/nylon 6/6

Samples	Stress yield (N/mm^2)	Young's modulus (N/mm^2)
Neat Nylon 6,6	0.90	52.82
ZnO(10wt)/nylon 6,6%	0.523	48.32
ZnO(20wt)/nylon 6,6%	0.66	47.33
ZnO(30wt)/nylon 6,6%	0.46	44.96

Table 1 illustrates the mechanical properties of both pure polymer & nanocomposites. The result presented that the Young's modulus and tensile strength of nanocomposites were drop off as increased the extent of ZnO NPs into nylon6/6. The reduction in mechanical properties of nanocomposite samples might be due to aggregation of ZnO NPs, which is generally happened by addition of high amount of fillers into matrix.

Photodegradation of alizarin red

Photocatalytic properties of Nylon and nanocomposites were performed via degrading alizarin red (AR) dye under UV-light. Figure 7a illustrates the UV/Vis spectra of alizarin red in aqueous media before and after UV-light irradiation

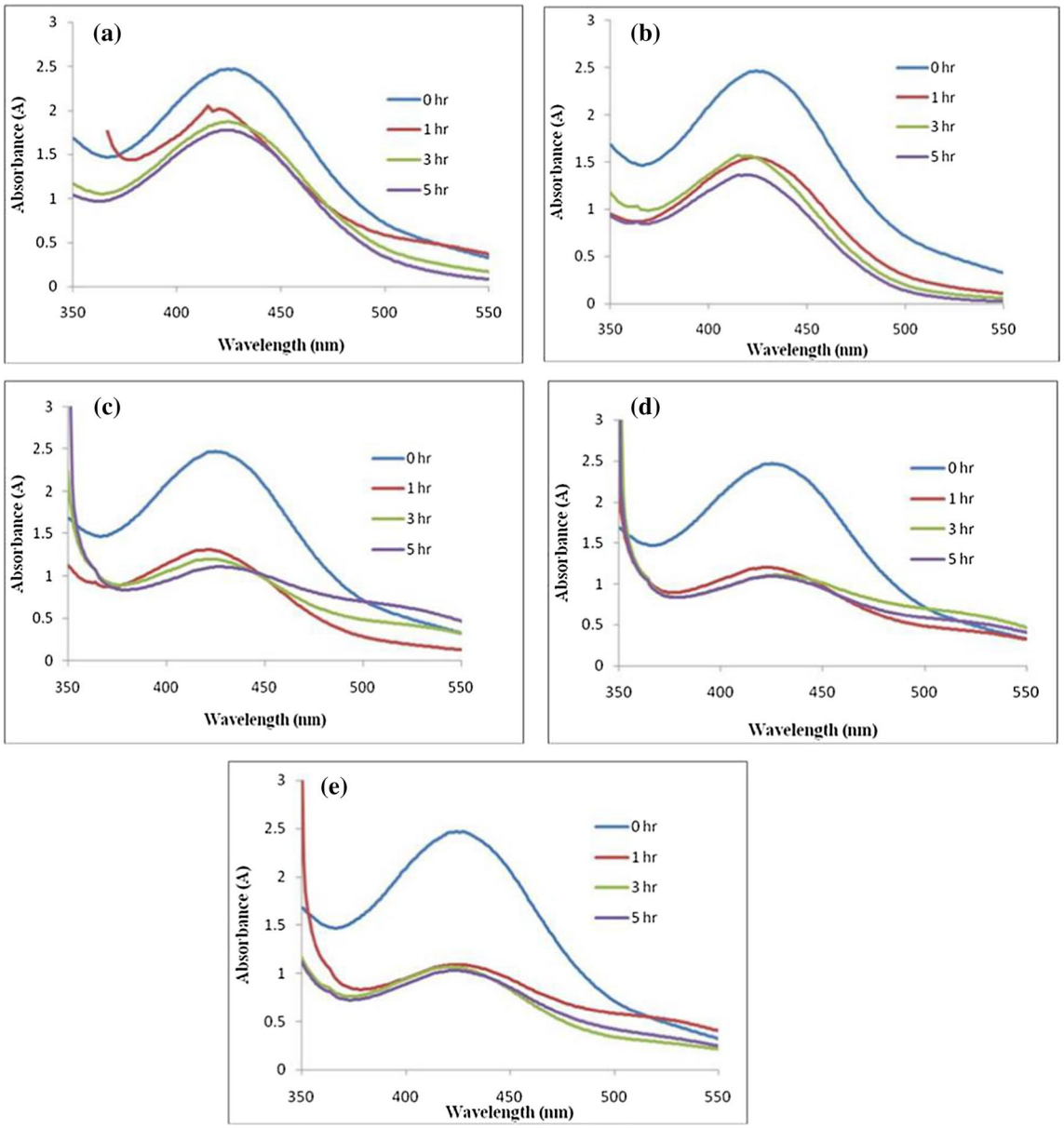

Fig. 7 UV/Vis spectra of AR photodegraded by **a** pure Nylon **b** 2%NPs/Nylon 6/6 **c** 10% NPs/Nylon 6/6 **d** 20%NPs/Nylon 6/6 **e** 30% ZnO/Nylon 6/6

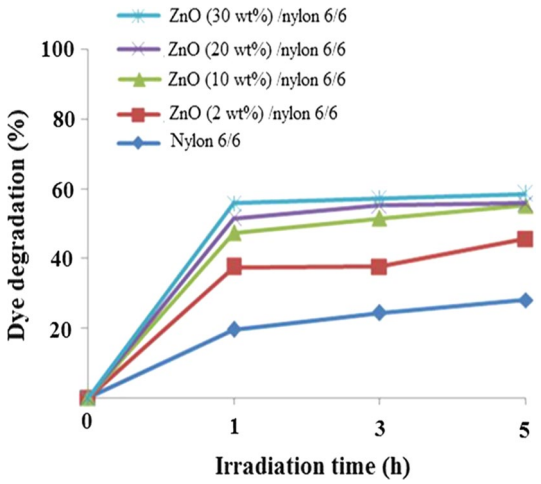

Fig. 8 Comparison of % degradation of dye by neat nylon 6/6 and nanocomposites samples

in the presence of pure nylon 6/6. The result shows that the photodegradation of alizarin red improved regularly with increasing irradiation time. Figure 7b–e shows the UV-Vis spectra of AR solution as degraded by 2, 10, 20 and 30% NPs/Nylon 6/6, respectively. The results show that dye degradation increases with increasing irradiation time. Recently nanoparticles incorporated polymers are used for the photodegradation of dyes (Saeed et al. 2018). The advantages of such photocatalysts over the other photocatalysts are the easy and complete separation, easy recoverability and washing. Figure 8 shows the comparison of % degradation of alizarin red dye photodegraded by all photocatalysts. Figure 8 shows that polymer containing high % of ZnO NPs degraded more dye within specific irradiation time, which might be due to high quantity of ZnO NPs, that act as a good semiconductor photocatalyst. The results show that pure Nylon 6/6 adsorbed about 28% dye within 5 h irradiation while

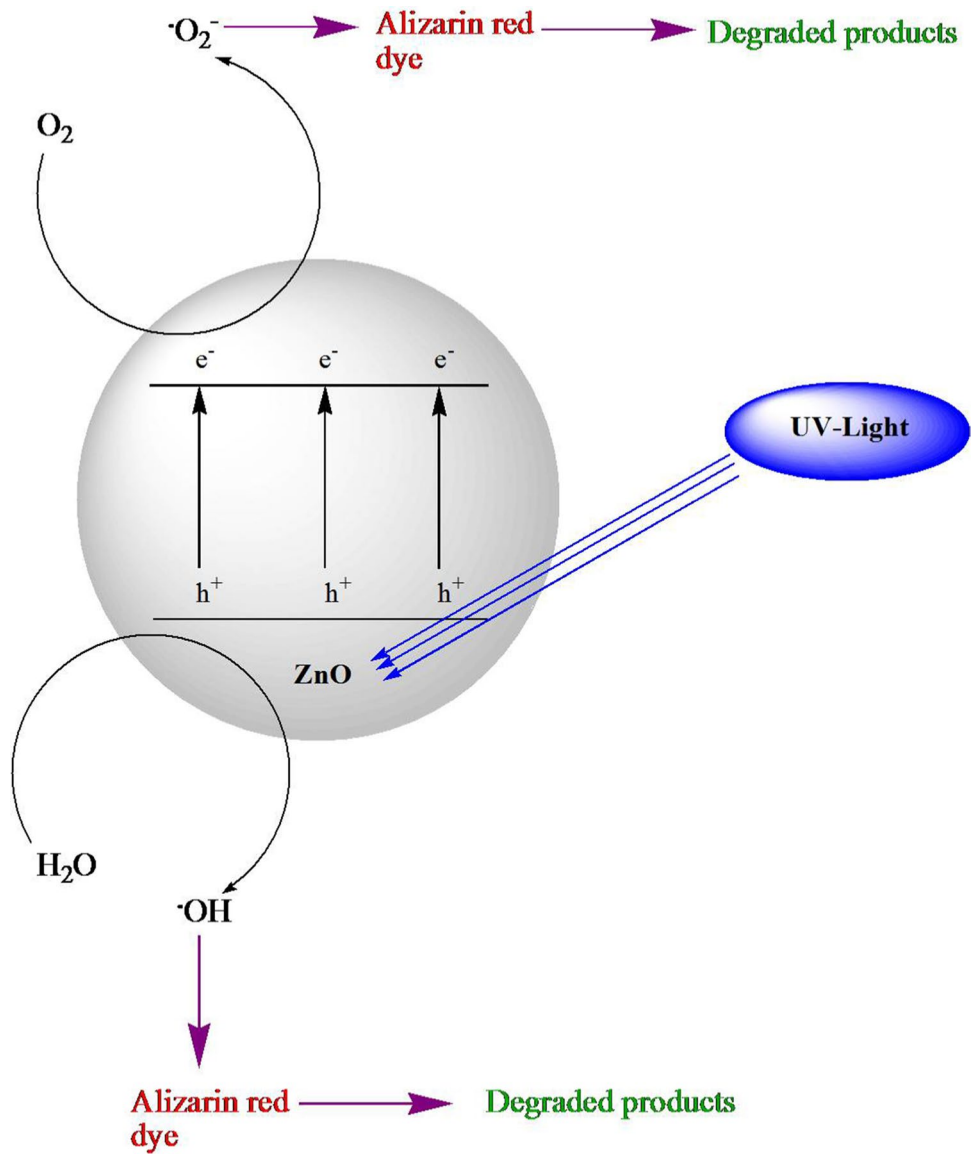

Fig. 9 Proposed mechanism for the photodegradation of AR dye photodegraded by ZnO

nanocomposite with high ZnO NPs (ZnO 30 wt% /nylon 6/6) degraded about 58.3% dye within the same irradiation time. Various studies are reported on the photodegradation of AR dye but these studies shows that they used pure metallic nanoparticles and their reaction conditions are complicated [Soodet al. 2014; Bharti and Bharati2018; Odeyemiet al. 2018). In contrast with these studies, our photocatalysts contain minute quantity of metal with full recoverability. The photodegradation of dyes achieved when UV-light falls on ZnO, which excite electrons (e^-) from valence band (VB) to the conduction band (CB), creating positively charged holes (h^+) in the VB. The e^- in the CB react with oxygen molecule (O_2) to produce superoxide anion radical ($^{\bullet}O_2^-$) while the h^+ in the VB reacts with H_2O molecules and generates hydroxyl radicals (•OH). These radicals generated are highly reactive and degraded dye molecules into simpler species such as CO_2 and H_2O (Khan et al. 2020). The proposed mechanism can be easily understood from Fig. 9.

Conclusion

It is concluded that the majority of ZnO NPs are present in dispersed form inside polymer but some aggregation of ZnO was also found in the polymer matrix. The spherulites of neat nylon 6,6 had distinct size while the size of spherulite in ZnO/nylon 6/6 is decreased regularly as increased the quantity of NPs into the nylon 6/6. The reduction in spherulites size might be due to the nucleation effect of NPs. The photodegradation study showed that NPs incorporation increased the photodegradation of dye as compared to neat polymer matrix.

Authors' contributions All the authors contributed equally in the work.

Funding This work was carried out with the financial support of Bacha Khan University.

Declaration

Conflict of interest The authors declare that they have no known competing financial interests or personal relationships that could have appeared to influence the work reported in this paper.

References

Alexandre M, Dubois P (2000) Polymer-layered silicate nanocomposites: preparation, properties and uses of a new class of materials. Mater Sci Eng 28:1–63

Ali N, Zhang B, Zhang H, Zaman W, Li W, Zhang Q (2014) Key synthesis of magnetic Janus nanoparticles using a modified facile method. Particuology 17:59–65

Ali N, Ali F, Khurshid R, Ikramullah AZ, Afzal A, Bilal M, Iqbal HMN, Ahmad I (2020) TiO_2 nanoparticles and epoxy-TiO_2nanocomposites: a review of synthesis, modification strategies, and photocatalytic potentialities. J Inorg Organomet Polym Mater 30:4829–4846

Ansari SP, Mohammad F (2016) Conducting nanocomposites of polyaniline/nylon 6,6/zinc oxide nanoparticles: preparation, characterization and electrical conductivity studies. Iran Polym J 25:363–371

Bharti DB, Bharati AV (2018) Photocatalytic degradation of Alizarin Red dye under visible light using ZnO & CdO nanomaterial. Optik 160(2018):371–379

Bizarria MTM, Giraldi ALFM, Carvalho CM, Velasco JI, dAvila MA, Mei LHI, (2007) Morphology and thermomechanical properties of recycled PET–organoclay nanocomposites. J Appl Polym Sci 104:1839–1844

Carter SA, Scott JC, Brock PJ (1997) Enhanced luminance in polymer composite light emitting devices. Appl Phys Lett 71:1145–1147

Chatterjee S, Guha N, Krishnan S, Singh AK, Mathur P, Rai DK (2020) Selective and recyclable congo Red dye adsorption by spherical Fe_3O_4 nanoparticles functionalized with 1,2,4,5-benzenetetracarboxylic acid. Sci Rep. https://doi.org/10.1038/s41598-019-57017-2

Długosz O, Banach M (2021) ZnO–SnO2–Sn nanocomposite as photocatalyst in ultraviolet and visible light. Appl Nanosci 11:1707–1719

Dunlop MJ, Bissessur R (2020) Nanocomposites based on graphene analogous materials and conducting polymers: a review. J Mater Sci 55:6721–6753

Feng Y, Yin J, Liu S, Wang Y, Li B, Jiao T (2020) Facile synthesis of Ag/Pd nanoparticle-loaded poly(ethylene imine) composite hydrogels with highly efficient catalytic reduction of 4-nitrophenol. ACS Omega 5:3725–3733

Garces JM, Moll DJ, Bicerano J, Fibiger R, McLeod DG (2000) Polymeric nanocomposites for automotive applications. Adv Mater 12:1835–1839

Gopiraman M, Saravanamoorthy S, Ullah S, Ilangovan A, Kim IS, Chung IM (2020) Reducing-agent-free facile preparation of Rh-nanoparticles uniformly anchored on onion-like fullerene for catalytic applications. RSC Adv 10:2545–2559

Halim NSA, Wirzal MDH, Bilad MR, Nordin NAHM, Putra ZA, Sambudi NS, Yusoff ARM (2019) Improving performance of electrospun nylon 6,6 nanofiber membrane for produced water filtration via solvent vapor treatment. Polymers. https://doi.org/10.3390/polym11122117

Hanemann T, Szabo DV (2010) Polymer-nanoparticle composites: from synthesis to modern applications. Materials 3:3468–3517

He J, Zhang Y, Guo Y, Rhodes G, Yeom J, Li H, Zhang W (2019) Photocatalytic degradation of cephalexin by ZnO nanowires under simulated sunlight: Kinetics, influencing factors, and mechanisms. Environ Int 132:105105

Hjiri M (2020) Highly sensitive NO_2 gas sensor based on hematite nanoparticles synthesized by sol–gel technique. J Mater Sci Mater El 31:5025–5031

Hu S, Yuan D, Liu Y, Zhao L, Guo H, Niu Q, Zong W, Liu R (2019) The toxic effects of alizarin red S on catalase at the molecular level. RSC Adv 9:33368–33377

Huszla K, Wysokowski M, Zgoła-Grześkowiak A, Staszak M, Janczarek M, Jesionowski T, Wyrwas B (2021) UV-light photocatalytic degradation of non-ionic surfactants using ZnO nanoparticles. Int J Environ Sci Technol. https://doi.org/10.1007/s13762-021-03160-1

Ibrahim S, Sultan M (2020) Superhydrophobic coating polymer/silica nanocomposites: part I synthesis and characterization as eco-friendly coating. Silicon 12:805–811

Iniestra-Galindo MG, Pérez-González J, Marín-Santibáñez BM, Balmori-Ramírez H (2019) Preparation at large-scale of polypropylene nanocomposites with microwaves reduced graphene oxide. Mater Res Express 6:105347

Irzhak VI, Dzhardimalieva GI, Uflyand IE (2019) Structure and properties of epoxy polymer nanocomposites reinforced with carbon nanotubes. J Polym Res 26:1–27

Iwamoto M, Kuroda K, Zaporojtchenko V, Hayashi S, Faupel F (2003) Production of gold nanoparticles-polymer composite by quite simple method. Eur Phys J D 24:365–367

Jadhav N, Kasisomayajula S, Gelling VJ (2020) Polypyrrole/metal oxides-based composites/nanocomposites for corrosion protection. Front Mater. https://doi.org/10.3389/fmats.2020.00095

Jasim SE, Jusoh MA, Hafiz M, Jose R (2016) Fabrication of superconducting YBCO nanoparticles by electrospinning. Procedia Eng 148:243–248

Jeon IY, Baek JB (2010) Nanocomposites derived from polymers and inorganic nanoparticles. Materials 3:3654–3674

Khan I, Khan I, Usman M, Imran M, Saeed K (2020) Nanoclay-mediated photocatalytic activity enhancement of copper oxide nanoparticles for enhanced methyl orange photodegradation. J Mater Sci Mater El 31:8971–8985

Kumar H, Manisha SP (2013) Synthesis and characterization of MnO_2 nanoparticles using co-precipitation technique. Iran J Chem Chem Eng 3:155–160

Khdary NH, Abdelsalam ME (2020) Polymer-silica nanocomposite membranes for CO_2 capturing. Arab J Chem 13:557–567

Li Y, Jian Z, Lang M, Zhang C, Huang X (2016) Covalently functionalized graphene by radical polymers for graphene based high-performance cathode materials. ACS Appl Mater Interfaces 8:17352–17359

Magdassi S, Bassa A, Vinetsky Y, Kamyshny A (2003) Silver nanoparticles as pigments for water-based ink-jet inks. Chem Mater 15:2208–2217

Mahalingam JL, Xu Z, Ren G, Rohn JL, Edirisinghe M (2015) Physio-chemical and antibacterial characteristics of pressure spun nylon nanofibres embedded with functional silver nanoparticles. Mater Sci Eng C 56:195–204

Mauri M, Collico V, Morelli L, Das P, Garcia I, Avila JP, Bellini M, Rotem R, Truffi M, Corsi F, Simonutti R, Liz-Marzan LM, Colombo M, Prosperi D (2020) MnO nanoparticles embedded in functional polymers as T_1 contrast agents for magnetic resonance imaging. ACS Appl Nano Mater 3:3787–3797

Mauro AD, Cantarella M, Nicotra G, Pellegrino G, Gulino A, Brundo MV, Privitera V, Impellizzeri G (2017) Novel synthesis of ZnO/PMMA nanocomposites for photocatalytic applications. Sci Rep 7:1–12

Meneghetti P, Qutubuddin S (2006) Synthesis, thermal properties and applications of polymer-clay nanocomposites. Thermochim Acta 442:74–77

Murugesan S, Scheibel T (2020) Copolymer/clay nanocomposites for biomedical applications. Adv Funct Mater 30:1908101

Nagaraju P, Puttaiah SH, Wantala K, Shahmoradi B (2020) Preparation of modified ZnO nanoparticles for photocatalytic degradation of chlorobenzene. Appl Water Sci. https://doi.org/10.1007/s13201-020-01228-w

Nawaz A, Khan A, Ali N, Ali N, Bilal M (2020) Fabrication and characterization of new ternary ferrites-chitosan nanocomposite for solar-light driven photocatalytic degradation of a model textile dye. Environ Technol Innov 20:101079

Nguyen TN, Moon J, Kim JJ (2020) Microstructure and mechanical properties of hardened cement paste including Nylon 66 nanofibers. Constr Build Mater 232:117134

Odeyemi OT, Owalude SO, Odebunmi EO (2018) Photocatalytic degradation of alizarin red dye in aqueous solution using titania-nickel and titania-cobalt nanocomposites. Ife J Sci 20:705–710

Ovcharenko EA, Seifalian A, Rezvova MA, Klyshnikov KY, Glushkova TV, Akenteva TN, Antonova LV, Velikanova EA, Chernonosova VS, Shevelev GY, Shishkova DK, Krivkina EO, Kudryavceva YA, Seifalian AM, Barbarash LS (2020) A new nanocomposite copolymer based On functionalized graphene oxide for development of heart valves. Sci Rep 10:1–14

Parlayici S, Avci A, Parlayici S, PehlivanE, (2019) Electrospinning of polymeric nanofiber (nylon 6,6/graphene oxide) for removal of Cr (VI): synthesis and adsorption studies. J Anal Sci Technol. https://doi.org/10.1186/s40543-019-0173-5

Prasert A, Sontikaew S, Sriprapai D, Chuangchote S (2020) Polypropylene/ZnO nanocomposites: mechanical properties, photocatalytic dye degradation, and antibacterial property. Materials. https://doi.org/10.3390/ma13040914

Rajakumar PR, Nanthini R (2013) Thermal and morphological behaviours of polybutylene terephthalate/polycarbonate blend nanocomposites. Int Lett Chem Phys A stron 4:15–36

Rehman R, Mahmud T (2013) Sorptive elimination of alizarin Red-S dye from water using citrullus lanatus peels in environmentally benign way along with equilibrium data modeling. Asian J Chem 25:5351–5356

Rezazadeh B, Sirousazar M, Chianeh VA, Kheiri F (2020) Polymer-clay nanocomposite hydrogels for molecular irrigation application. J Appl Polym Sci 137:48631

Russo M, Iervolino G, Vaiano V (2021) W-poped ZnO Photocatalyst for the degradation of glyphosate in aqueous solution. Catalysts 11:234

Saeed K, Khan I (2014) Preparation and properties of single-walled carbon nanotubes/poly (butylenes terephthalate) nanocomposites. Iran Polym J 23:53–58

Saeed K, Khan I, Ahmad Z, Khan B (2018) Preparation, analyses and application of cobalt–manganese oxides/nylon 6,6 nanocomposites. Polym Bull 75:4657–4669

Saeed K, Khan I, Park SY (2015) TiO_2/Amidoxime modified Polyacrylonitrile nanofibers and its application for the Photodegradation of Methyl blue in Aqueous Medium. Desalin Water Treat 54:3146–3151

Schmidt G, Malwitz MM (2003) Properties of polymer–nanoparticle composites. Curr Opin Colloid Interface Sci 8:103–108

Selvam GG, Sivakumar K (2015) Phycosynthesis of silver nanoparticles and photocatalytic degradation of methyl orange dye using silver (Ag) nanoparticles synthesized from Hypneamusciformis (Wulfen) J.V. Lamouroux Applnanosci 5:617–622

Sinha T, Ahmaruzzaman M, Bhattacharjee A (2014) A simple approach for the synthesis of silver nanoparticles and their application as a catalyst for the photodegradation of methyl violet 6B dye under solar irradiation. J Environ Chem Eng 2:2269–2279

Soltani RDC, Haghighat Z (2016) Visible light photocatalysis of a textile dye over ZnO nanostructures covered on natural diatomite. Turk J Chem 40:454–466

Sood S, Mehta SK, Umar A, Kansal SK (2014) The visible light-driven photocatalytic degradation of Alizarin red S using Bi-doped TiO_2 nanoparticles. New J Chem 38:3127–3136

Sovizi MR, MirzakhanibS, (2020) A chemiresistor sensor modified with lanthanum oxide nanoparticles as a highly sensitive and selective sensor for dimethylamine at room temperature. New J Chem 44:4927–4934

Wang H, Xie C, Zhang W, Cai S, Yang Z, Gui Y (2007) Comparison of dye degradation efficiency using ZnO powders with various size scales. J Hazard Mater 141:645–652

Wu C, Cai R, Zhao T, Wu L, Zhang L, Jin J, Xu L, Li P, Li T, Zhang M, Du F (2020) Hyaluronic acid-functionalized gadolinium oxide nanoparticles for magnetic resonance imaging-guided radiotherapy of tumors. Nanoscale Res Lett 15:1–2

Xu Z, Mahalingam S, Rohn JL, Ren G, Edirisinghe M (2015) Physiochemical and antibacterial characteristics of pressure spun nylon nanofibres embedded with functional silver nanoparticles. Mater Sci Eng C 56:195–204. https://doi.org/10.1016/j.msec.2015.06.003

Xu Y, Ray G, Abdel-Magid B (2006) Thermal behavior of single-walled carbon nanotube polymer–matrix composites. Compos Part A Appl Sci Manuf 37:114–121

Yanilmaz M, Zhu J, Lu Y, Ge Y, Zhang X (2017) High-strength, thermally stable nylon 6,6 composite nanofiber separators for lithium-ion batteries. J Mater Sci 52:5232–5241

Yang Y, Ali N, Khan A, Khan S, Khan S, Khan H, Xiaoqi S, Ahmad W, Uddin S, Ali N, Bilal M (2021) Chitosan-capped ternary metal selenide nanocatalysts for efficient degradation of Congo red dye in sunlight irradiation. Int J BiolMacromol 167:169–181